This paper is published as part of a *Dalton Transactions* themed issue on:

Metal-catalysed Polymerisation

Guest Editors: Barbara Milani and Carmen Claver
University of Trieste, Italy and Universitat Rovira i Virgili, Tarragona, Spain

Published in issue 41, 2009 of *Dalton Transactions*

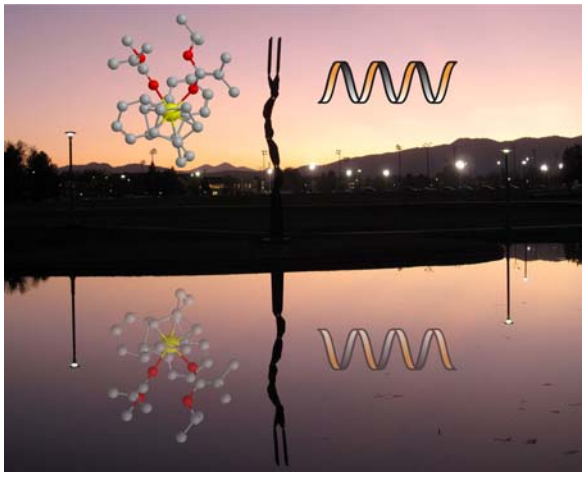

Image reproduced with permission of Eugene Chen

Articles published in this issue include:

PERSPECTIVES:

HOT PAPERS:

Visit the *Dalton Transactions* website for more cutting-edge organometallic and catalysis research
www.rsc.org/dalton

Synthesis, structure and ethylene polymerisation behaviour of vanadium(IV and V) complexes bearing chelating aryloxides †

Damien Homden,[a] Carl Redshaw,*[a] Lee Warford,[a] David L. Hughes,[a] Joseph A. Wright,[a] Sophie H. Dale[b] and Mark R. J. Elsegood[b]

Received 28th January 2009, Accepted 15th May 2009
First published as an Advance Article on the web 7th July 2009
DOI: 10.1039/b901810g

The reaction of [V(N*p*-tolyl)Cl_3] with the sulfur-bridged diphenol ligand 2,2′-thiobis(4,6-di-*tert*-butylphenol), {2,2′-S[4,6-(*t*-Bu)$_2$$C_6H_2$OH]$_2$} ($LSH_2$) afforded the complexes [V$(LS)_2$] (**1**) and [$VOCl_3$(MeCN)$_2$][H_3N*p*-tolyl] (**2**). Complex **2** could also be prepared directly from [V(N*p*-tolyl)Cl_3] and 'wet' acetonitrile. Reaction of [V(N*p*-tolyl)(O*t*-Bu)$_3$] with LSH_2 afforded [VO(μ_2-OH)(LS)]$_2$·6(MeCN) (**3**), whilst reaction of [VO(O*n*-Pr)$_3$] with 2,2′-sulfinylbis(4,6-di-*tert*-butylphenol), {2,2′-SO_2[4,6-(*t*-Bu)$_2$$C_6H_2$OH]$_2$} ($LSO_2H_2$), afforded [V$(LSO_2)_2$]·MeCN (**4**). The reaction of [VO(O*i*-Pr)$_3$] with the ethylidene-bridged diphenol 2,2′-ethylidenebis(4,6-di-*tert*-butylphenol), {2,2′-CH_3CH[4,6-(*t*-Bu)$_2$$C_6H_2$OH]$_2$} ($LH_2$) afforded the hydroxyl bridged complexes [(VOL)$_2$(μ_2-OH)(μ_2-O*i*-Pr)] (**5**) (major product) and [VO(μ_2-OH)(L)]$_2$·4(MeCN) (**6**) (minor product). In general, we find that controlled hydrolysis of [V(NAr)(O*n*-Pr)$_3$] (Ar = *p*-ClC_6H_4, *p*-$OCNC_6H_4$ or *p*-tolyl) in the presence of LH_2 reproducibly led to the vanadyl complex [VO(μ-O*n*-Pr)L]$_2$·2(MeCN) (**7**), in which the *n*-propoxide bridges both unexpectedly lie above the V_2O_2 plane. Reaction of the linear triphenol 2,6-bis(3,5-di-*tert*-butyl-2-hydroxybenzyl)-4-*tert*-butylphenol, [$ArCH_2Ar^1CH_2Ar$] (Ar = 4,6-di-*tert*-butylphenol; Ar^1 = 4-*tert*-butylphenol) (L^1H_3), and [VO(O*n*-Pr)$_3$] afforded the complex [VOL^1]$_2$·3(MeCN) (**8**), whilst reaction of [V(N*p*-tolyl)(O*i*-Pr)$_3$] with the related methylene-bridged linear triphenol 2,6-bis(3,5-di-*tert*-butyl-2-hydroxybenzyl)-4-methylphenol, [$ArCH_2Ar^2CH_2Ar$] (L^2H_3) (Ar^2 = 4-methylphenol), gave {[V(μ_2-O)(N*p*-tolyl)][VO(O*i*-Pr)]L^2}$_2$·1.5(MeCN) (**9**). The crystal structures of **1** to **9** are reported. Complexes **1**–**4** and **7**–**9** were screened as pro-catalysts for the polymerisation of ethylene in the presence of the co-catalyst dimethylaluminium chloride (DMAC) and the re-activator ethyltrichloroacetate (ETA). All are highly active ethylene polymerisation catalysts with activities covering the range 2000 to 90 000 g $mmol^{-1}$ h^{-1} bar^{-1}, and these results are discussed in terms of the ligands present at vanadium in the pro-catalyst. Complex **3** has also been screened for ethylene/propylene copolymerisation.

Introduction

The last couple of years have seen an upsurge of interest in vanadium-based systems for α-olefin polymerisation.[1] Very high activities and thermal stability have been observed for a number of systems, particularly where the vanadium pro-catalyst is combined with an organoaluminium chloride co-catalyst such as dimethylaluminium chloride (DMAC).[2] The presence of the reactivator ethyltrichloroacetate (ETA) has also proved to be beneficial in most of these vanadium systems.[3] Despite the fact that the active species remains somewhat of a mystery, it is clear that the use of certain ligands at vanadium leads to enhanced catalytic performance. Amongst those affording the highest activities to-date are phenoxyimine systems reported by Fujita *et al.*,[4] and bis(benzimidazole)amines utilized by the group of Gibson.[5] Aryloxides are also proving to be useful ancillary ligands in this field of study,[6] and Nomura has reported a number of imido/aryloxide systems,[7] whilst we have previously communicated a number of vanadyl complexes bearing chelating bi- or tri-dentate phenolate ligands, the structures of which are shown in Scheme 1.[2a]

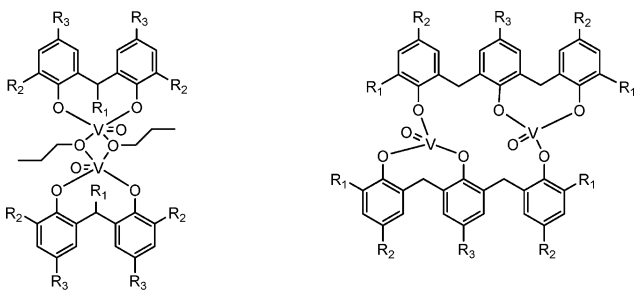

Scheme 1

Given the high activities observed for such vanadyl systems, we have extended our studies to include the use of other bi- and

[a]*Energy Materials Laboratory, School of Chemistry, University of East Anglia, Norwich, UK NR4 7TJ. E-mail: carl.redshaw@uea.ac.uk*
[b]*Chemistry Department, Loughborough University, Loughborough, Leicestershire, UK LE11 3TU*

† CCDC reference numbers 718343–718350. For crystallographic data in CIF or other electronic format see DOI: 10.1039/b901810g

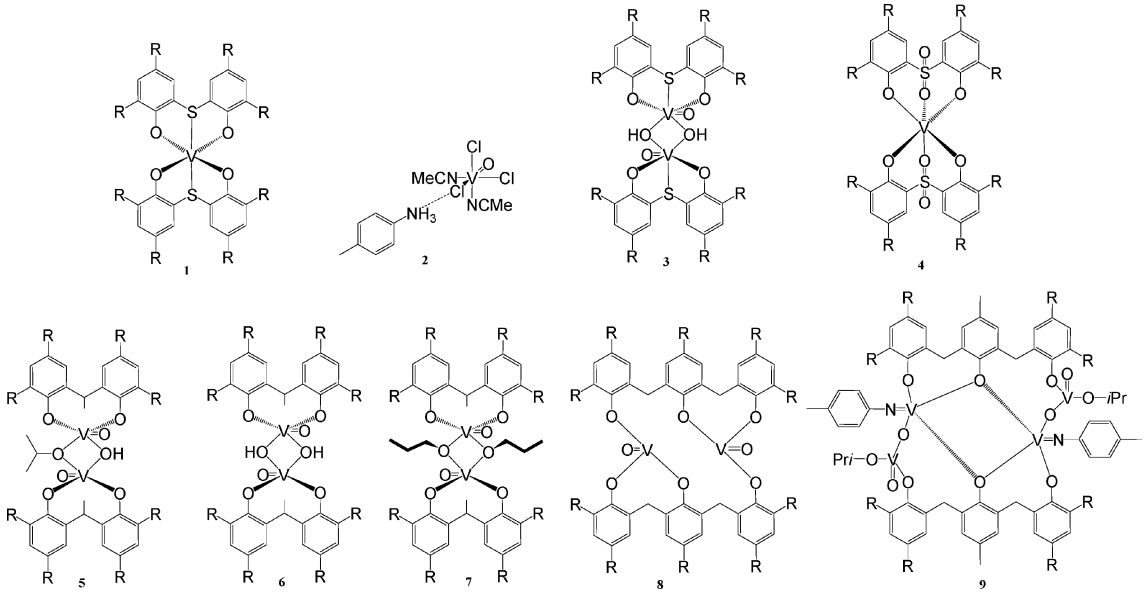

Scheme 2 Vanadium complexes **1–9** (R = *t*-butyl).

tri-phenols, including ligands with bridging sulfur and sulfonylene groups (Scheme 2). Takaoki and Miyatake have previously utilised a thiobis(phenoxy) vanadyl pro-catalyst to polymerise propylene (activities $\leq$ 2000 g mmol^{-1} h^{-1} bar^{-1}),[8] whilst Janas and Sobota have used 2,2′-thiobis{4-(1,1,3,3-tetramethylbutyl)phenol} in conjunction with [$VCl_3(THF)_3$] and [$VO(OEt)_3$] to prepare dimeric vanadium(III) and (V) complexes, respectively, which when supported on $MgCl_2$ and activated with aluminium alkyls were efficient ethylene polymerization catalysts (activities $\leq$ 11 708 g mmol^{-1} h^{-1} bar^{-1}).[9] Two recent reports have also appeared in the literature concerning the coordination of sulfur-bridged diphenols to high-valent vanadium, and those synthetic/structural results will be compared with ours reported here.[10] In the patent literature, there is mention of [V(NAr)(diphenolate)Cl]-type pro-catalysts, where the diphenolate can be methylene or sulfur bridged, and the imido group possesses a number of electron-withdrawing groups.[11]

We also note that mono- and bi-nuclear vanadium(V) alkoxides are biologically attractive,[12] and that [VOL(OR)]-type complexes have been shown to undergo hydrolysis to afford bi-nuclear [$VOL]_2$ (L = ONO tridentate ligand) species.[13]

Results and discussion

Use of sulfur-bridged diphenols

The reaction of [V(N*p*-tolyl)Cl_3] with the sulfur-bridged diphenol pro-ligand 2,2′-thiobis(4,6-di-*tert*-butylphenol), {2,2′-S[4,6-(*t*-Bu)$_2C_6H_2OH]_2$} (LSH_2) afforded a mixture of the complexes [$V(LS)_2$] (**1**) and [$VOCl_3(MeCN)_2$][H_3N*p*-tolyl] (**2**) in isolated yields of 47 and 17%, respectively. Complex **2** could also be prepared directly from [V(N*p*-tolyl)Cl_3] and 'wet' acetonitrile in > 90% yield. Both brown **1** and green/brown **2** can be readily recrystallised from acetonitrile affording crystals suitable for X-ray diffraction. Complex **1** is the same as that reported by Chaudhuri *et al.*, where it was obtained from the reaction of the ligand LSH_2 with [$VCl_3(THF)_3$] in the presence of Et_3N.[9b] In the formation of anilinium salt **2**, the imido group of [V(N*p*-tolyl)Cl_3] has been protonated and lost from the metal centre. The structure of **2** is shown in Fig. 1, with bond lengths and angles given in Table 1. The vanadium centre is distorted octahedral with a *mer* arrangement of chloride ligands. The oxo group exerts a strong *trans* influence on the acetonitrile [V(1)–N(2) 2.3990(16) *cf.* V(1)–N(1) 2.1369(16) Å]. There are four unique N–H $\cdots$ Cl hydrogen bonds (Fig. 2, Table 2) involving all three hydrogen atoms of the anilinium salt; this results in chains that run along the *b* axis with only weak interactions between the chains.

Table 1 Selected bond lengths (Å) and angles (°) for **2**

Bond lengths/Å	
V(1)–O(1)	1.5893(13)
V(1)–Cl(1)	2.3647(6)
V(1)–Cl(2)	2.3586(5)
V(1)–Cl(3)	2.4257(6)
V(1)–N(1)	2.1369(16)
V(1)–N(2)	2.3990(16)
Bond angles/°	
O(1)–V(1)–Cl(1)	88.07(5)
O(1)–V(1)–Cl(2)	99.08(5)
O(1)–V(1)–Cl(3)	97.92(6)
O(1)–V(1)–N(1)	92.75(7)
O(1)–V(1)–N(2)	174.52(7)
N(1)–V(1)–Cl(2)	168.17(5)
Cl(1)–V(1)–Cl(3)	162.53(2)
V(1)–N(1)–C(1)	166.71(15)
V(1)–N(2)–C(3)	174.79(17)

The reaction of [V(N*p*-tolyl)(O*t*-Bu)$_3$] with LSH_2 afforded the purple complex [$VO(\mu_2$-OH)(LS)]$_2$ (**3**) in good yield (*ca.* 70%). Crystals of **3**·6MeCN suitable for X-ray diffraction were grown from a 'hot' (heated to reflux for several minutes with a heat-gun) solution of acetonitrile on cooling to ambient temperature. The structure, shown in Fig. 3, is similar to the complex [$VO(\mu_2$-OH)(LS)]$_2$·2(MeCN) reported by Cornman *et al.* for the product of the reaction between [VO(O*i*-Pr)$_3$] and LSH_2 in acetonitrile.[9a]

Table 2 Hydrogen bonds for **2** (Å and °)

D–H···A	*d*(D–H)	*d*(H···A)	*d*(D···A)	∠(DHA)
N(3)–H(3A)···Cl(1′)	0.91	2.51	3.2847(17)	144
N(3)–H(3A)···Cl(2′)	0.91	2.51	3.1826(17)	131
N(3)–H(3B)···Cl(3″)	0.91	2.39	3.2998(16)	174
N(3)–H(3C)···Cl(3)	0.91	2.47	3.3352(17)	160

Symmetry operations for equivalent atoms: ′ $x, y + 1, z$, ″ $1 - x, y + \frac{1}{2}, 1 - z$.

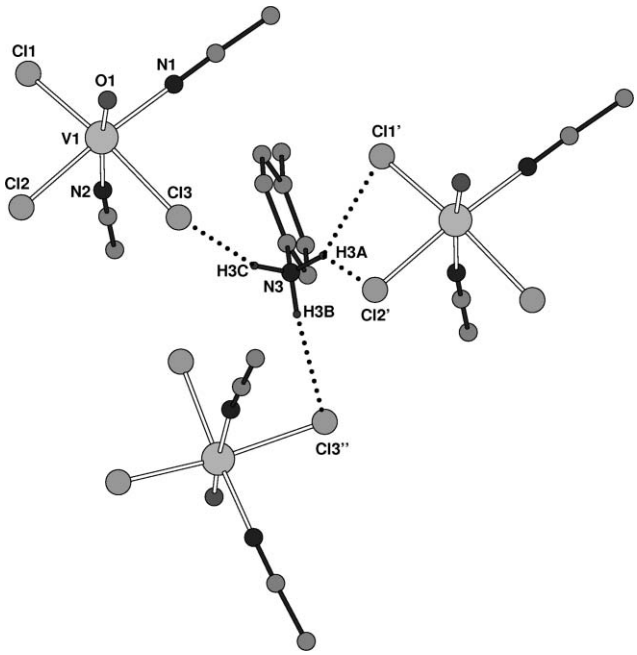

Fig. 1 CAMERON representation of the structure of **2** showing spheres of arbitrary size; hydrogen atoms (except H3a, H3b and H3c) have been omitted for clarity.

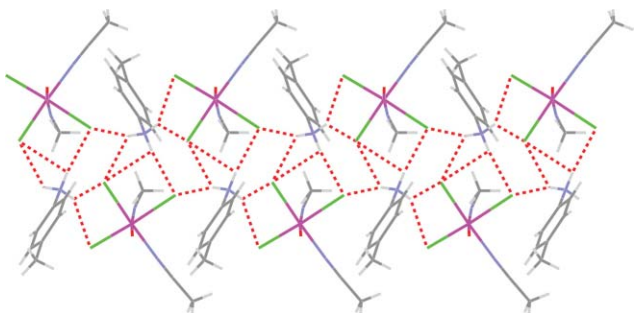

Fig. 2 Chains of **2** formed by hydrogen bonds. View is down the crystallographic *a*-axis.

Bond lengths and angles for **3**·6(MeCN) and the Cornman complex are compared in Table 3. Both complexes lie on centres of symmetry and contain *facially* bound LS ligands in which the sulfur is *trans* to an oxo ligand. However in **3**·6(MeCN) the hydroxide bridges are slightly asymmetric, with one of the three unique acetonitrile solvent molecules hydrogen-bonded to each bridge.

The reaction of [VO(O*n*-Pr)$_3$] with 2,2′-sulfonylenebis(4,6-di-*tert*-butylphenol), {2,2′-SO_2[4,6-(*t*-Bu)$_2$C$_6$H$_2$OH]$_2$} (LSO_2H_2), afforded brown [V(LSO_2)$_2$] (**4**) in *ca.* 33% yield. Crystals of **4**·MeCN suitable for X-ray diffraction were grown from a saturated solution

Table 3 Selected bond lengths (Å) and angles (°) for **3**·6(MeCN) and the Cornman structure.[9a] Symmetry operations ′: for complex **3**·6(MeCN) = $1 - x, 1 - y, 1 - x$, and for Cornman's complex = $2 - x, 1 - y, -z$

3·6(MeCN)		Cornman structure [VO(μ$_2$-OH)(LS)]$_2$·4(MeCN)	
Bond lengths/Å			
V(1)–O(1)	1.8409(15)	V(1)–O(3)	1.838(2)
V(1)–O(2)	1.8472(16)	V(1)–O(4)	1.861(2)
V(1)–O(3)	1.9624(15)	V(1)–O(2)	1.973(2)
V(1)–O(3′)	1.9736(16)	V(1)–O(2′)	1.973(2)
V(1)–O(4)	1.5904(17)	V(1)–O(1)	1.593(2)
V(1)–S(1)	2.7620(7)	V(1)–S(1)	2.7953(7)
Bond angles/°			
O(4)–V(1)–O(1)	99.30(8)	O(1)–V(1)–O(3)	97.89(8)
O(4)–V(1)–O(2)	97.81(8)	O(1)–V(1)–O(4)	99.79(8)
O(4)–V(1)–O(3)	103.57(8)	O(1)–V(1)–O(2)	101.85(8)
O(4)–V(1)–O(3′)	102.82(8)	O(1)–V(1)–O(2′)	103.76(8)
O(4)–V(1)–S(1)	172.90(6)	O(1)–V(1)–S(1)	172.33(7)
O(1)–V(1)–O(3)	154.24(7)	O(3)–V(1)–O(2)	157.27(7)
O(2)–V(1)–O(3′)	156.72(7)	O(4)–V(1)–O(2′)	154.12(7)
V(1)–O(3)–V(1′)	106.79(7)	V(1)–O(2)–V(1′)	106.50(8)

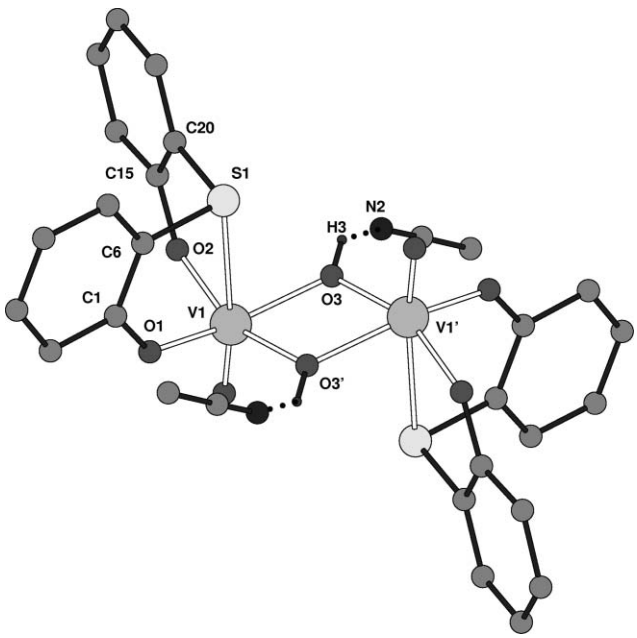

Fig. 3 CAMERON representation of the structure of **3**·6MeCN showing spheres of arbitrary size; alkyl groups, hydrogen atoms (except H3) and four non-coordinated molecules of acetonitrile have been omitted for clarity.

of acetonitrile at ambient temperature. The structure, shown in Fig. 4, reveals a distorted octahedral vanadium centre bound by two *facially* coordinated LSO_2 ligands. Two molecules of **4**·MeCN are present in the asymmetric unit, and have similar geometric parameters (Table 4).

Use of ethylidene-bridged diphenols

The reaction of [VO(O*i*-Pr)$_3$] with the ethylidene-bridged diphenol 2,2′-ethylidenebis(4,6-di-*tert*-butylphenol), {2,2′-CH_3CH[4,6-(*t*-Bu)$_2$C$_6$H$_2$OH]$_2$} (LH_2) afforded the hydroxyl bridged

Table 4 Selected bond lengths (Å) and angles (°) for **4**·MeCN

Bond lengths/Å			
V(1)–O(1)	2.0931(18)	V(2)–O(11)	2.0846(19)
V(1)–O(2)	1.816(2)	V(2)–O(10)	1.8235(19)
V(1)–O(3)	1.8765(19)	V(2)–O(9)	1.8644(19)
V(1)–O(5)	1.8755(18)	V(2)–O(13)	1.8687(18)
V(1)–O(6)	1.8520(19)	V(2)–O(14)	1.8365(19)
V(1)–O(7)	2.100(2)	V(2)–O(15)	2.0868(19)
Bond angles/°			
O(1)–V(1)–O(2)	84.23(8)	O(10)–V(2)–O(11)	85.72(8)
O(1)–V(1)–O(3)	89.10(8)	O(9)–V(2)–O(11)	90.54(8)
O(1)–V(1)–O(5)	174.94(8)	O(11)–V(2)–O(13)	174.22(8)
O(1)–V(1)–O(6)	85.31(8)	O(11)–V(2)–O(14)	83.93(8)
O(1)–V(1)–O(7)	87.77(8)	O(11)–V(2)–O(15)	86.51(7)
O(2)–V(1)–O(6)	164.64(9)	O(10)–V(2)–O(14)	166.83(9)
O(3)–V(1)–O(7)	176.20(8)	O(9)–V(2)–O(15)	176.84(8)

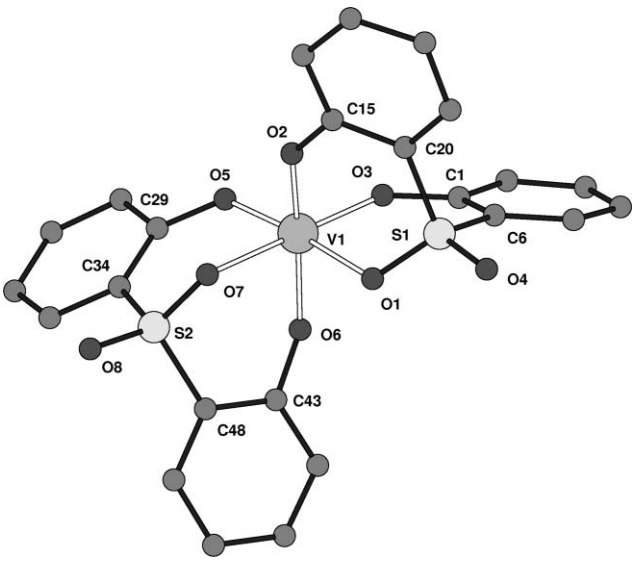

Fig. 4 CAMERON representation of the structure of one of the two independent molecules of **4**·MeCN in the asymmetric unit, showing spheres of arbitrary size; the solvent molecule, alkyl groups and hydrogen atoms have been omitted for clarity.

complexes [(VOL)$_2$(μ_2-OH)(μ_2-O*i*-Pr)] (**5**) (major product) and [VO(μ_2-OH)(L)]$_2$ (**6**) (minor product). Both complexes can be readily recrystallised from saturated solutions of acetonitrile affording crystals suitable for X-ray crystallography. Complex **5** (Fig. 5, Table 5) lies on a 2-fold symmetry axis which runs through O(5) and H(5) with O(1) and the attached *i*-Pr group disordered close to the axis. The geometry at each vanadium centre can be described as distorted square-based pyramidal, and the centres are linked *via* asymmetric OH/O*i*-Pr bridging. The difference in the bridging ligands is best illustrated by the angles subtended at each oxygen, V(1)–O(5)–V(1′) 110.11(8) *cf.* V(1)–O(1)–V(1′) 108.07(10)°. The chelating ligand forms an 8-membered metallocycle adopting a boat conformation, with a bite angle of 93.53(5)°, somewhat smaller than that found for the monomeric vanadyl complex {VOCl[2,2′-CH$_2$(4-Me-6-*t*-BuC$_6$H$_2$O)$_2$]} [106.9(2)°],[14] but comparable to that found for the dimeric structure [VO(O*n*-Pr)L]$_2$ [94.49(10)°].[2a]

Table 5 Selected bond lengths (Å) and angles (°) for **5** and **6**·4(MeCN). Symmetry operations ′: for complex **5** = $\frac{1}{2} - x, y, 1 - z$, and for **6**·4(MeCN) = $2 - x, 1 - y, -z$

5		**6**·4(MeCN)	
Bond lengths/Å			
V(1)–O(1)	1.858(6)	V(1)–O(1)	1.9752(11)
V(1)–O(2)	1.5861(13)	V(1)–O(2)	1.5840(11)
V(1)–O(3)	1.8048(10)	V(1)–O(4)	1.8054(10)
V(1)–O(4)	1.8109(10)	V(1)–O(3)	1.8131(10)
V(1)–O(5)	1.9621(9)	V(1)–O(1′)	1.9559(11)
Bond angles/°			
O(1)–V(1)–O(2)	95.02(17)	O(2)–V(1)–O(1)	105.07(5)
O(2)–V(1)–O(3)	105.77(6)	O(2)–V(1)–O(4)	104.92(5)
O(2)–V(1)–O(4)	103.03(7)	O(2)–V(1)–O(3)	104.13(5)
O(2)–V(1)–O(5)	112.15(5)	O(2)–V(1)–O(1′)	104.35(5)
O(1)–V(1)–O(4)	155.47(11)	O(1)–V(1)–O(3)	148.73(5)
O(3)–V(1)–O(5)	141.49(4)	O(4)–V(1)–O(1′)	148.59(5)
V(1)–O(1)–V(1′)	108.07(10)	V(1)–O(1)–V(1′)	107.28(5)
V(1)–O(5)–V(1′)	110.11(8)	V(1)–O(1′)–V(1′)	107.28(5)
O(3)–V(1)–O(4)	93.53(5)	O(3)–V(1)–O(4)	94.26(5)

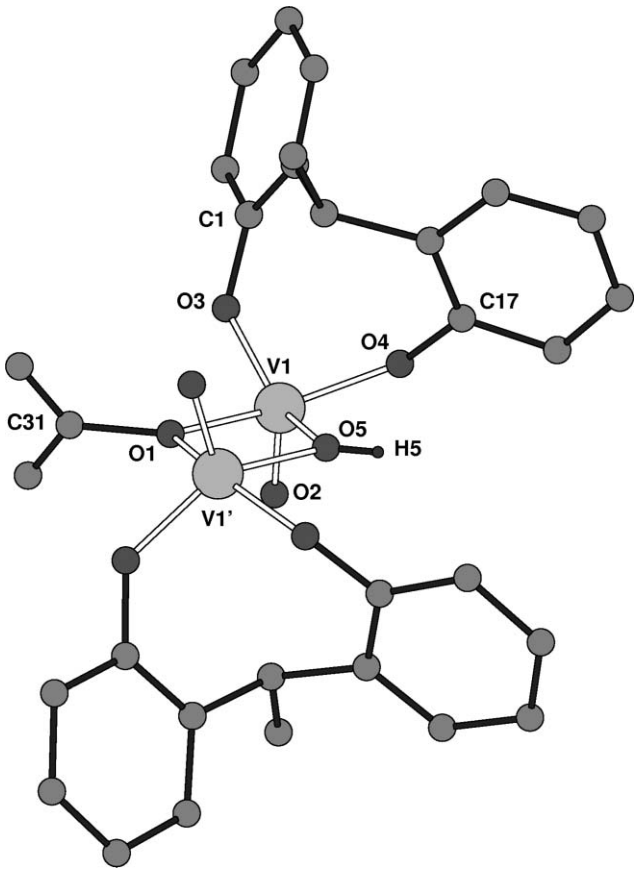

Fig. 5 CAMERON representation of the structure of **5** showing spheres of arbitrary size; *tert*-butyl groups and hydrogen atoms (except H5) have been omitted for clarity.

The IR spectrum of **5** contains a strong band at 999 cm^{-1} assigned to the ν(V=O) group, and broader bands at 3175 and 3482 cm^{-1} assigned to ν(OH). In complex **6**·4(MeCN) (Fig. 6, Table 5), the dimer sits about an inversion centre and,

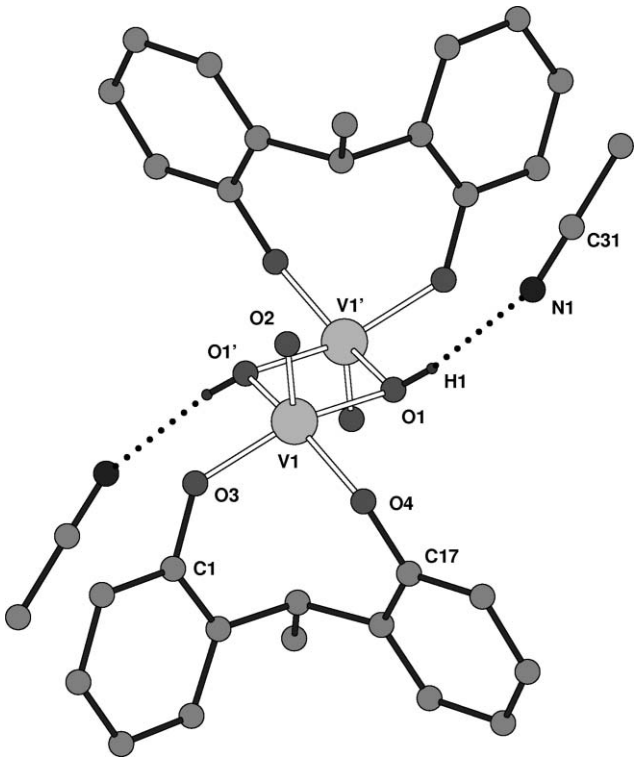

Fig. 6 CAMERON representation of the structure of **6**·(4MeCN) showing spheres of arbitrary size; hydrogen atoms (except H1 and H1′), *tert*-butyl groups and two molecules of unbound acetonitrile per dimer have been omitted for clarity.

as in **3**, there are acetonitrile ligands bound through O–H···N hydrogen bonds to the slightly asymmetric hydroxide bridges. The other acetonitrile ligands associated with **6** simply fill the voids in the lattice. Each vanadyl centre is square-based pyramidal, with the vanadyl group at the apex. The chelating ligand forms an eight-membered metallocycle adopting a boat conformation [bite angle = 94.26(5)°]. The V···V distance is 3.166 Å. The IR spectrum contains a strong band at 1014 cm^{-1} assigned to the ν(V=O) group, and broader bands at 3165 and 3253 cm^{-1} assigned to ν(OH). The ease of formation of **5** and **6** seems to be related to the use and sensitivity of the vanadyl tris-isopropoxide starting material. Under similar conditions, using the analogous *n*-propoxide starting material, we have not observed any hydroxide bridged species. Interestingly, Cornman *et al.* also employed [VO(O*i*-Pr)$_3$] in the reaction with LSH_2 which afforded either [VO(LS)(μ-OEt)]$_2$ (from ethanol) or as mentioned earlier in our discussions of compound **3**, the hydroxide-bridged complex [VO(LS)(μ-OH)]$_2$ (from acetonitrile), the formation of the latter (and a related structure derived from a selenium-bridged diphenol) was also reported by Chaudhuri *et al.*[9b]

Interestingly, the product obtained from the 'controlled' hydrolysis (one equivalent of H_2O added) of [V(NAr)(O*n*-Pr)$_3$]/LH_2 (Ar = *p*-ClC_6H_4, *p*-$OCNC_6H_4$ or *p*-tolyl), namely [VO(μ-O*n*-Pr)L]$_2$ (**7b**), always contained (as characterised by single-crystal X-ray diffraction for all three reactions using the differing Ar groups) *n*-Pr groups on the same side of the V_2O_2 plane (Fig. 7b), which is in contrast to that previously reported for the structure resulting from the reaction of [VO(O*n*-Pr)$_3$] and LH_2 (Fig. 7a).[2a] The geometrical parameters (Table 6) associated with both structures are, as expected, similar, with only slight differences observed for the angles about each vanadium centre. ^{1}H NMR solution spectra showed two isomers to be present in an approx. 4 to 1 ratio (major to minor); in toluene-d_8, C_6D_6 or CD_3CN there was little change in the appearance of the spectra over the temperature range 20 to 80 °C. ^{51}V NMR spectra showed only trace signs of minor hydrolysed (OH-bridged) product present in each case.

Use of methylene-bridged triphenols

Reaction of the linear triphenol 2,6-bis(3,5-di-*tert*-butyl-2-hydroxybenzyl)-4-*tert*-butylphenol, [$ArCH_2Ar^1CH_2Ar$] (Ar = 4,6-di-*t*-butylphenol; Ar^1 = 4-*t*-butylphenol) (L^1H_3), and [VO(O*n*-Pr)$_3$] afforded the complex [VOL^1]$_2$ (**8**) in *ca.* 45% yield. The complex can be readily recrystallised from acetonitrile, and the structure of **8**·3(MeCN) (Fig. 8, Table 7) is similar to that we previously reported for the complex derived from the related triphenol ligand [$ArCH_2Ar^2CH_2Ar$] (L^2H_3) (Ar^2 = 4-methylphenol).[2a] In particular, the ligand binds in an unsymmetrical fashion, *viz.* η^2-coordination to one approximately tetrahedral vanadium atom (with angles in the range 107.89(9) to 112.53(8)°), with the resulting eight-membered ring having a boat conformation with a bite angle of 108.15(8)° (*cf.* 106.7(2)° for [VO(O*n*-Pr)L]$_2$). A two-fold symmetry axis runs through the middle of the central cavity.

Interestingly, when we switched to the use of the isopropoxide starting material [V(N*p*-tolyl)(O*i*-Pr)$_3$], reaction with the triphenol L^2H_3 led to the isolation of the complex {[V(μ$_2$-O)(N*p*-tolyl)][VO(O*i*-Pr)]L^2}$_2$ (**9**·1.5MeCN), containing four vanadium centres (Fig. 9, Table 8). Here, V(3) and V(4) are approximately tetrahedral, whilst V(1) and V(2) are best described as trigonal bipyramidal with the axial positions in each occupied by a near-linear imido group and the bridging central phenolate oxygen of an L^2 ligand. The two different vanadium environments are clearly distinguishable in the ^{51}V NMR spectrum [δ: −452 ($\omega_{1/2}$ 4000), −515 ($\omega_{1/2}$ 1200)]. The molecule shows approximate two-fold symmetry.

Ethylene polymerisation

Complexes **1–4** and **7–9** (all samples were dried *in vacuo* for 12 h prior to use) were screened as pro-catalysts for ethylene polymerisation in the presence of a variety of organoaluminium co-catalysts (DMAC, MAO and Me_3Al), and in the presence of the re-activator ethyltrichloroacetate (ETA). Under the conditions employed, only the combination of procatalyst/DMAC/ETA gave significant catalytic activities (see Tables 9–11, Fig. 10).

Pro-catalysts **1** and **4**, both of which contain no vanadyl group, showed similar behaviour with activities in the region of 21 000 g $mmol^{-1}$ h^{-1} bar^{-1} affording high molecular weight polymers (217 000 and 244 000, respectively). The absence of a chelating ligand (run 2) led to a dramatic loss of catalytic activity, with observed values down to *ca.* 2000 g $mmol^{-1}$ h^{-1} bar^{-1}. However, when a combination of vanadyl group and chelating diphenolate ligand (either methylene or sulfur-bridged) was present, observed activities were extremely high (≥ 62 000 g $mmol^{-1}$ h^{-1} bar^{-1}). Similarly, use of the methylene bridged triphenolate ligands in combination with vanadyl (**8**) or vanadyl/vanadium imido groups (**9**) afforded very high activities, with that observed from the use of **9** being about 90 000 g $mmol^{-1}$ h^{-1} bar^{-1}. The polymers

Table 6 Selected bond lengths (Å) and angles (°) for 'up-down'-[VO(O*n*-Pr)L]$_2$ (**7a**·MeCN) and **7b**·2(MeCN)

'up-down'-[VO(O*n*-Pr)L]$_2$ (**7a**·MeCN)		**7b**·2(MeCN)			
Bond lengths/Å					
V(1)–O(1)	1.973(3)	V(1)–O(1)	1.976(4)	V(2)–O(2)	1.974(4)
V(1)–O(2)	1.583(3)	V(1)–O(8)	1.568(4)	V(2)–O(5)	1.567(4)
V(1)–O(3)	1.802(2)	V(1)–O(6)	1.797(4)	V(2)–O(4)	1.814(4)
V(1)–O(4)	1.815(2)	V(1)–O(7)	1.802(4)	V(2)–O(3)	1.810(3)
V(1)–O(1′)	1.973(3)	V(1)–O(2)	1.967(4)	V(2)–O(1)	1.977(4)
Bond angles/°					
O(3)–V(1)–O(4)	94.49(10)	O(6)–V(1)–O(7)	93.47(17)	O(4)–V(2)–O(3)	94.91(16)
V(1)–O(3)–C(1)	141.3(2)	V(1)–O(6)–C(37)	140.8(3)	V(2)–O(4)–C(12)	139.5(3)
V(1)–O(4)–C(17)	136.6(2)	V(1)–O(7)–C(45)	137.7(3)	V(2)–O(3)–C(4)	137.9(3)
O(1)–V(1)–O(1A)	72.35(12)	O(1)–V(1)–O(2)	71.35(15)	O(2)–V(2)–O(1)	71.21(15)

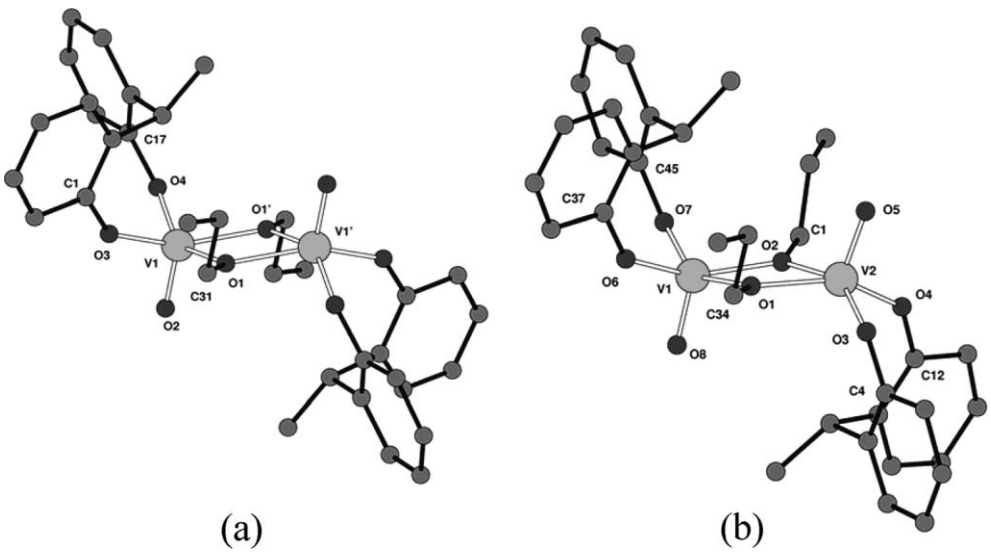

Fig. 7 CAMERON representation of the structures of (a) **7a**·MeCN [2a] and (b) **7b**·2(MeCN) showing spheres of arbitrary size; *tert*-butyl groups, acetonitrile molecules and hydrogen atoms have been omitted for clarity.

afforded by both catalyst systems derived from the use of **8** and **9** displayed very similar properties with respect to molecular weight and polydispersities (Table 9 and Fig. 10, runs 4 and 5), suggesting that similar active species were generated upon the addition of DMAC.

More comprehensive screening was carried out upon **1** (Table 10). Over the temperature range 0–80 °C, the activity of **1** was found to peak at *ca.* 60 °C (run 4); above this temperature the activity was found to decrease slightly, with a concomitant drop in the molecular weight of the resulting polymer (Table 10, runs 1–5). A steady increase in activity, similar to that of the niobium pro-catalysts bearing similar ligands,[15] was found upon increasing the concentration of DMAC (runs 6–10); such an increase was found to lower the PDI of the resulting polymer, whilst the weight of the polymer ($\bar{M}_w$) remained relatively constant. The use of other co-catalysts, such as TMA and MAO, led to a significant drop in polymerisation activity. A similar drop in activity was also observed upon removal of ETA; such a trend has been observed previously for vanadium-based catalysis.[1–3]

Complex **3** was screened under more robust conditions at both 25 °C and 80 °C—see Table 11. At the elevated temperature (80 °C, run 2), there is a 10-fold increase in activity. This pro-catalyst was also screened for ethylene/propylene copolymerization at 25 °C, and was found to have an activity of *ca.* 20 000 g mmol^{-1} h^{-1} bar^{-1} with 13.2% propylene incorporation.

In conclusion, we have structurally characterised a number of high-valent vanadium complexes bearing chelating aryloxide ligands with CH_2, CH(Me), S or SO_2 bridges. Screening for ethylene polymerization in the presence of DMAC/ETA indicates that the chelate ligand is clearly beneficial to the catalytic activity of the system. Activity is further increased by the additional presence of vanadyl or vanadium imido groups.

Experimental

General

All manipulations were carried out under an atmosphere of dinitrogen using standard Schlenk and cannula techniques or in a conventional nitrogen-filled glove-box. Solvents were refluxed over

Table 7 Selected bond lengths (Å) and angles (°) for **8**·3(MeCN) and the analogue $[VOL^2]_2$[2a]

8		$[VOL^2]_2$			
Bond lengths/Å					
V(1)–O(1)	1.5954(18)	V(1)–O(7)	1.592(6)	V(2)–O(8)	1.587(6)
V(1)–O(1A)	1.7823(16)	V(1)–O(1)	1.779(5)	V(2)–O(2)	1.752(5)
V(1)–O(1B)	1.7707(16)	V(1)–O(5)	1.748(5)	V(2)–O(3)	1.754(5)
V(1)–O(1C)	1.7760(17)	V(1)–O(6)	1.722(5)	V(2)–O(4)	1.760(5)
Bond angles/°					
O(1)–V(1)–O(1A)	109.85(9)	O(7)–V(1)–O(1)	110.1(3)	O(8)–V(2)–O(2)	107.6(3)
O(1)–V(1)–O(1B)	107.89(9)	O(7)–V(1)–O(5)	107.7(3)	O(8)–V(2)–O(3)	109.1(3)
O(1)–V(1)–O(1C)	110.00(9)	O(7)–V(1)–O(6)	110.3(3)	O(8)–V(2)–O(4)	110.4(3)
O(1A)–V(1)–O(1B)	112.53(8)	O(1)–V(1)–O(5)	112.4(2)	O(2)–V(2)–O(3)	106.7(2)
O(1B)–V(1)–O(1C)	108.15(8)	O(5)–V(1)–O(6)	107.7(2)	O(3)–V(2)–O(4)	109.7(2)
O(1A)–V(1)–O(1C)	108.39(8)	O(1)–V(1)–O(6)	108.6(2)	O(2)–V(2)–O(4)	113.1(2)

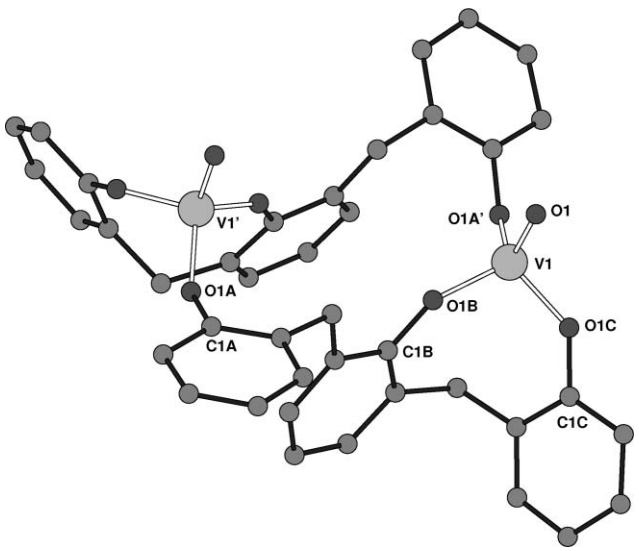

Fig. 8 CAMERON representation of the structure of **8**·3(MeCN) showing spheres of arbitrary size; alkyl groups, three molecules of acetonitrile and hydrogen atoms have been omitted for clarity.

Table 8 Selected bond lengths (Å) and angles (°) for **9**·1.5(MeCN)

Bond lengths/Å			
V(1)–N(1)	1.6625(15)	V(2)–N(2)	1.6631(15)
V(1)–O(6)	1.7853(12)	V(2)–O(3)	1.7924(12)
V(1)–O(5)	1.8944(12)	V(2)–O(2)	1.9015(12)
V(1)–O(11)	1.8456(13)	V(2)–O(12)	1.8450(13)
V(1)–O(2)	2.1547(12)	V(2)–O(5)	2.1604(12)
V(3)–O(7)	1.5869(15)	V(4)–O(9)	1.5855(15)
V(3)–O(1)	1.7850(13)	V(4)–O(4)	1.7803(13)
V(3)–O(11)	1.7394(13)	V(4)–O(12)	1.7490(13)
V(3)–O(8)	1.7446(14)	V(4)–O(10)	1.7419(15)
Bond angles/°			
N(1)–V(1)–O(6)	101.08(6)	N(2)–V(2)–O(3)	101.35(7)
N(1)–V(1)–O(5)	95.27(6)	N(2)–V(2)–O(2)	94.82(7)
N(1)–V(1)–O(11)	100.30(7)	N(2)–V(2)–O(12)	99.99(7)
N(1)–V(1)–O(2)	158.47(6)	N(2)–V(2)–O(5)	158.26(6)
O(5)–V(1)–O(6)	103.29(5)	O(2)–V(2)–O(3)	104.74(6)
O(5)–V(1)–O(11)	136.67(6)	O(2)–V(2)–O(12)	134.81(6)
V(1)–N(1)–C(75)	174.01(14)	V(2)–N(2)–C(82)	170.99(14)
O(7)–V(3)–O(1)	110.64(7)	O(9)–V(4)–O(4)	110.21(7)
O(7)–V(3)–O(11)	108.61(7)	O(9)–V(4)–O(12)	109.26(7)
O(7)–V(3)–O(8)	106.90(8)	O(9)–V(4)–O(10)	108.08(8)
O(1)–V(3)–O(8)	109.25(7)	O(4)–V(4)–O(10)	108.17(7)
O(1)–V(3)–O(11)	110.92(6)	O(4)–V(4)–O(12)	110.42(6)
V(3)–O(11)–V(1)	141.62(8)	V(4)–O(12)–V(2)	141.72(8)
V(1)–O(5)–V(2)	110.40(5)	V(1)–O(2)–V(2)	110.36(5)

Table 9 Ethylene polymerisation runs for **1**, **2**, **4**, **8** and **9**

Run	Catalyst	Activity/g mmol^{-1} h^{-1} bar^{-1}	$\bar{M}_w$/g mol^{-1}	M_n/ g mol^{-1}	PDI	mp/°C
1	**1**	20 480	217 000	81 700	2.7	132.9
2	**2**	2 120	256 000	60 100	4.3	134.3
3	**4**	21 640	244 000	111 000	2.2	134.4
4[a]	**8**	89 840	173 000	43 800	4.0	135.0
5[b]	**9**	36 660	178 000	40 900	4.3	133.7

[a] 10 min run time. [b] 15 min run time. All runs completed with 0.05 µmol of [V], 40 000 equivalents DMAC and 0.1 mL ETA in 50 mL toluene at 50 °C for 30 min.

an appropriate drying agent, and distilled and degassed prior to use. Elemental analyses were performed by the microanalytical services of the School of Chemical Sciences & Pharmacy at UEA or at London Metropolitan University. EPR spectroscopy was performed on an X-band ER200-D spectrometer (Bruker Spectrospin) interfaced to an ESP1600 computer and fitted with a liquid helium flow cryostat (ESR-900; Oxford Instruments). NMR spectra were recorded on a Varian VXR 400 S spectrometer at 400 MHz or a Gemini at 300 MHz (^{1}H), 105.1 MHz (^{51}V) at 298 K; chemical shifts are referenced to the residual protio impurity of the deuterated solvent. IR spectra (nujol mulls, KBr windows) were recorded on Perkin-Elmer 577 and 457 grating spectrophotometers. The complexes [V(N*p*-tolyl)(OR)$_3$] (R = *n*-Pr, *i*-Pr, *t*-Bu) and [VO(OR)$_3$] (R = Et, *n*-Pr) were prepared as described in the literature.[16,17] [VO(O*i*-Pr)$_3$] was a gift from the former Inorg Tech. Ltd. The ligand LSH_2 was prepared as previously reported,[18] while LSO_2H_2 was prepared *via* the hydrogen peroxide oxidation of LSH_2.[8]

All other chemicals were obtained commercially and used as received unless stated otherwise.

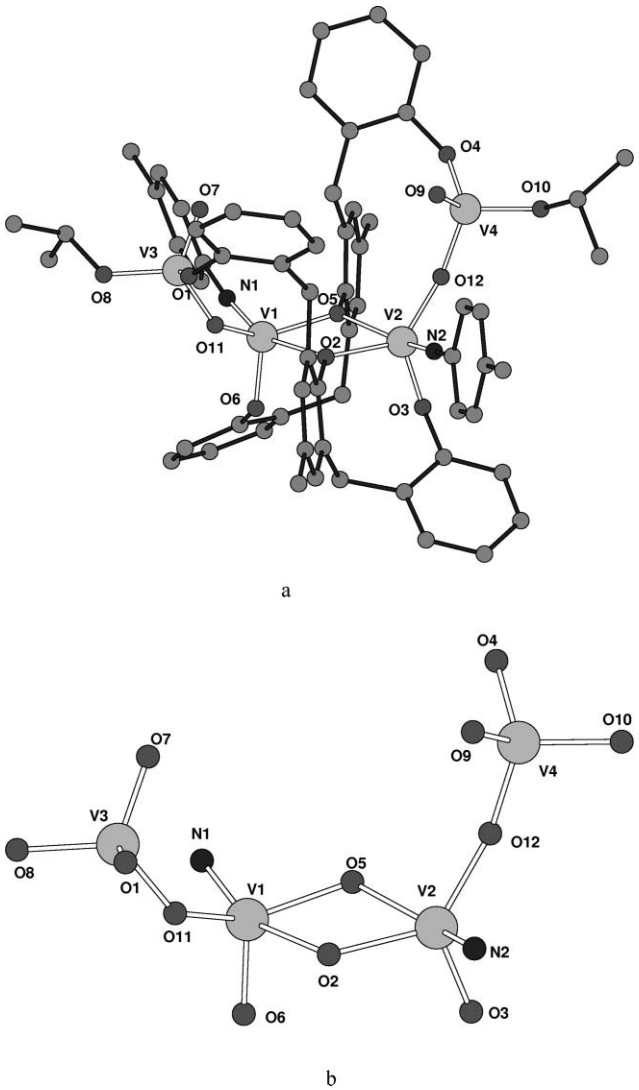

Fig. 9 (a) CAMERON representation of the structure of **9**·1.5(MeCN) showing spheres of arbitrary size. (b) View of the core of **9**·1.5(MeCN). Solvent molecules, *tert*-butyl groups and hydrogen atoms have been omitted for clarity.

Table 10 Ethylene screening for **1**

Run	[Al] : [V]	T/°C	Activity/g mmol^{-1} h^{-1} bar^{-1}	$\bar{M}_w$/g mol^{-1}	M_n/g mol^{-1}	PDI
1	20 000	0	2 760	464 000	126 000	3.7
2	20 000	25	4 920	360 000	160 000	2.2
3	20 000	45	11 320	332 000	115 000	2.9
4	20 000	60	33 040	188 000	71 400	2.6
5	20 000	80	28 280	54 200	25 500	2.1
6	10 000	25	5 880	367 000	97 800	3.8
7	20 000	25	6 310	—	—	—
8	30 000	25	7 480	—	—	—
9	40 000	25	7 760	—	—	—
10	50 000	25	8 240	386 000	169 000	2.3

All runs completed with 5 μmol of [V], DMAC and 0.1 mL ETA in 50 mL of toluene for 15 min.

Synthesis of [V(LS)$_2$] (1). [V(N*p*-tolyl)Cl$_3$] (1.00 g, 3.81 mmol) and LSH$_2$ (1.69 g, 3.82 mmol) were refluxed in toluene for 12 h.

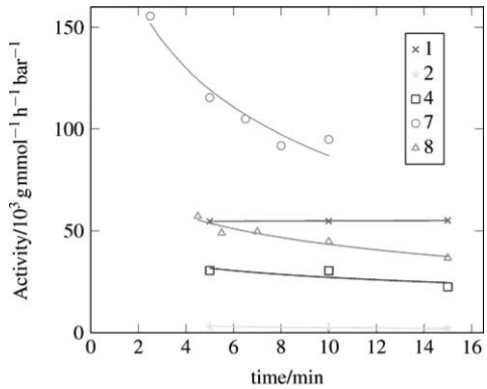

Fig. 10 Lifetime graph of ethylene polymerisation for **1**, **2**, **4**, **8** and **9**. Conditions: 50 ml toluene at 50 °C, 0.1 mL ETA, 40 000 equivalents of DMAC, 0.05 μmol of [V].

Table 11 Ethylene and ethylene/propylene screening for **3** under more robust conditions

Run	T/°C	Activity/g mmol^{-1} h^{-1} bar^{-1}	C_3 content (mol%)
1	25	7 500	n/a
2	80	72 600	n/a
3	25	19 800	13.2

Conditions: toluene 250 mL, 250 equiv. of DMAC, 0.5 mmol ETA, 15 min.

Upon cooling, the solvents were removed *in vacuo* and the residue was extracted into acetonitrile. Standing at ambient temperature for 3–4 d afforded **1** as green/brown prisms, yield: 0.83 g, 47% together with {[VOCl$_3$(NCMe)$_2$]·[*p*-tolylNH$_3$]} (**2**) (0.12 g, 17%). For **1**: mp > 250 °C. $C_{56}H_{80}O_4S_2V$ (932.26) calcd (found) C 72.2 (72.1) H 8.7 (8.6). *m*/*z* (MALDI): 932 (M$^+$). IR (cm^{-1}): 2735 s, 2619 m, 2601 s, 2358 s, 2286 s, 2260 m, 1562 m, 1507 m, 1260 m, 1089 m, 1053 m, 1024 m, 975 m, 865 m, 801 w, 798 w, 740 s, 659 m. Magnetic moment $\mu = 1.62\mu_B$. EPR (toluene, 298 K): $g_{iso} = 1.98$, $A_{iso} = 69$ G, (toluene, 10 K) $g_\perp = 1.99$, $A_\perp = 67$ G, $g_\parallel = 1.96$, $A_\parallel = 185$ G.

Alternative synthesis of {[VOCl$_3$(NCMe)$_2$]·[*p*-tolylNH$_3$]} (2). [V(N*p*–tolyl)Cl$_3$] (1.00 g, 3.81 mmol) was refluxed in degassed acetonitrile (50 mL). Cooling of the solution to ambient temperature and removal of solvent *in vacuo* afforded **2** as a brown solid. Yield: 1.30 g, 94%. mp 95 °C. $C_{11}H_{16}ON_3Cl_3V$ (363.57) calcd (found): C 36.3 (35.8) H 4.4 (5.1) N 11.6 (11.1)%. ^{1}H NMR (C_6D_6, 400 MHz) δ: 7.24 (2 H, d $^3J_{HH}$ 4.8 Hz, tolyl-*H*), 6.38 (2 H, d, $^3J_{HH}$ 4.8 Hz, tolyl-*H*), 3.83 (3 H, bs, N*H*$_3$), 1.82 (3 H, s, tolyl-*Me*), 0.59 (6 H, bs, *Me*CN).^{51}V (C_6D_6, 105.1 MHz) δ: −384.24 ($\omega_{1/2}$ 448). *m*/*z* (EI+): 255 ([VOCl$_3$(MeCN)$_2$]$^+$), (EI−): 108 (H$_3$N*p*-tolyl$^-$). IR (cm^{-1}): 2726 m, 2360 m, 2321 m, 2293 m, 1602 bm, 1557 w, 1260 s, 1094 bm, 1017 bm, 865 w, 802 w, 725 w.

Synthesis of [VO(μ$_2$-OH)(LS)]$_2$·6(MeCN) (3). [V(N*p*-tolyl)(O*t*-Bu)$_3$] (0.85 g, 2.26 mmol) with LSH$_2$ (1.00 g, 2.26 mmol) were refluxed in toluene (30 mL) for 12 h. Following removal of volatiles *in vacuo*, the residue was extracted into 'hot' acetonitrile (30 mL), affording as a purple crystalline solid **3**·6(MeCN) on prolonged standing at ambient temperature. Yield 0.99 g, 68%. $C_{58}H_{85}NO_8S_2V_2$ (sample dried *in vacuo* for 12 h, −5MeCN, 1090.5) calcd (found): C 63.9 (64.0) H 7.9 (8.7) N 1.3 (1.3)%. IR: 3413 bs, 1716 w, 1636 w, 1583 w, 1515 w, 1362 s, 1284 s, 1260 s, 1202 w,

1137 m, 1100 s, 1021 m, 996 m, 916 w, 880 m, 839 s, 806 s, 750 m, 722 w, 636 m. ^{1}H NMR (C_6D_6, 400 MHz) δ: 7.53 (s, 2 H, Ar-*H*), 7.01 (s, 2 H, Ar-*H*), 3.69 (bs, 2 H, O*H*), 1.30 (bs, 18 H, C(CH_3)$_3$), 1.24 (bs, 18 H, C(CH_3)$_3$).

Synthesis of [V(LSO$_2$)$_2$]·MeCN (4). [VO(O*n*-Pr)$_3$] (0.24 mL, 1.06 mmol) and LSO_2H_2 (1.00 g, 2.11 mmol) were refluxed in toluene for 12 h. Upon cooling the solvents were removed *in vacuo* and the residue was extracted into acetonitrile. Standing at ambient temperature for 3–4 d afforded **4**·MeCN as brown prisms. Yield: 350 mg, 33%. mp > 250 °C. $C_{56}H_{80}O_8S_2V$ (sample dried *in vacuo* for 12 h, –MeCN, 996.33) calcd (found) C 67.5 (67.7) H 8.1 (8.3). *m*/*z* (MALDI): 996 (M^+). IR (cm^{-1}): 3359 bs, 3122 bs, 2730 s, 2609 s, 2349 s, 2288 s, 2260 s, 1563 s, 1510 s, 1260 m, 1090 bm, 1019 m, 985 m, 866 m, 801 m, 722 s, 660 s. Magnetic moment μ = 1.71μ_B. EPR (toluene, 298 K): g_{iso} = 1.97, A_{iso} = 70 G, (toluene, 10 K) $g_\perp$ = 1.99, $A_\perp$ = 65 G, $g_\parallel$ = 1.96, $A_\parallel$ = 186 G.

Synthesis of [(VOL)$_2$(μ$_2$-OH)(μ$_2$-O*i*-Pr)] (5) and [VO(μ$_2$-OH)(L)]$_2$·4(MeCN) (6). To LH_2 (2.00 g, 4.58 mmol) in toluene (40 mL) was added [VO(O*i*-Pr)$_3$] (1.08 mL, 4.58 mmol). The dark brown solution was refluxed for 12 h, volatiles were removed *in vacuo*, and the residue was extracted into 'hot' acetonitrile (30 mL). Prolonged standing (1–2 d) at ambient temperature afforded dark brown crystals of **5** (1.74 g, 35%) and dark red crystals of **6**·4(MeCN) (yield (< 5%). Complex **5** can also be recrystallised from dichloromethane at 0 °C. $C_{63}H_{96}O_8V_2$ (1083.28) calcd (found) C 69.8 (70.4) H 8.9 (9.0). IR (cm^{-1}): 3646 m, 3170 bm, 2724 m, 2673 m, 1649 w, 1589 m, 1415 w, 1261 m, 1234 m, 1199 m, 1149 m, 1106 bm, 1005 bm, 922 w, 904 w, 880 m, 797 m, 759 m, 634 m. ^{1}H NMR ($CDCl_3$, 400 MHz) δ: 7.38–7.16 (3× m, 8 H, aryl*H*), 5.45 (bm, 1 H, *J* not observed*, C*H*(CH$_3$)$_2$), 4.91 (q, 2 H, $^3J_{HH}$ 7.0 Hz, C*H*C(CH$_3$)), 1.57 (d, 6 H, 7.0 Hz, CHC(CH_3)), 1.37 (s, 36 H, C(CH_3)$_3$), 1.26 (s, 36 H, C(CH_3)$_3$), 1.23 (d, 3 H, *J* not observed*, CH(CH_3)$_2$). μ-OH not observed. * = cooling to –20 °C had no effect. ^{51}V ($CDCl_3$, 105.1 MHz) δ:–410.80 ($\omega_{1/2}$ 500).

For **6**: *m*/*z* (FAB): 1066.6 (MH^+ – 3MeCN – OH), 1049.6 (MH^+ – 3MeCN – 2OH), 1034.7 (MH^+ – 3MeCN – 2O). ^{1}H NMR ($CDCl_3$, 400 MHz) δ: 7.38–7.16 (3 × m, 8 H, aryl*H*), 4.92 (q, 2 H, $^3J_{HH}$ 7.0 Hz, C*H*C(CH$_3$)), 1.57 (d, 6 H, 7.0 Hz, CHC(CH_3)), 1.37 (s, 36 H, C(CH_3)$_3$), 1.26 (s, 36 H, C(CH_3)$_3$). μ-OH not observed. ^{51}V ($CDCl_3$, 105.1 MHz) δ: –410.91 ($\omega_{1/2}$ 438). IR (cm^{-1}): 3489 w, 2620 w, 1595 w, 1507 w, 1411 w, 1363 m, 1261 s, 1216 w, 1201 w, 1154 w, 1095 bs, 1017 bs, 930 w, 905 w, 880 w, 800 bs, 725 w. $C_{65}H_{97.5}N_{2.5}O_8V_2$ (sample dried *in vacuo* for 12 h, –1.5MeCN, 1144.0) calcd (found): C 68.2 (65.1) H 8.6 (8.5) N 3.1 (3.1).[19]

Synthesis of [VO(O*n*-Pr)L]$_2$·2(MeCN) (7b). [V(NAr)(O*n*-Pr)$_3$] (Ar = *p*-tolyl) (1.53 g, 4.59 mmol), LH_2 (2.00 g, 4.58 mmol) and H_2O (0.08 mL, 4.44 mmol) were refluxed in toluene (40 mL) for 12 h. Upon cooling, volatiles were removed *in vacuo*, and the residue was taken up in 'hot' MeCN (30 mL) and filtered whilst still warm. Upon cooling to ambient temperature, red/brown prisms of **7**·2(MeCN) formed. Further crops of **7**·2(MeCN) can be obtained by concentration and cooling of the mother liquor. Yield: 2.19 g, 79%. *m*/*z* (MALDI): 1005 (M^+ – 2MeCN – 2PrOH). IR (cm^{-1}): 1745 w, 1592 m, 1262 m, 1233 m, 1199 m, 1172 m, 1147 m, 1112 m, 1031 m, 1002 s, 981 s, 921 m, 895 w, 881 m, 853 s, 797 m, 779 m, 758 m, 727 w, 693 w, 653 w, 635 m, 613 w, 574 s, 542 m. $C_{66}H_{102}O_8V_2$·2(C_2H_3N) (sample dried *in vacuo* for 12 h, –MeCN, 1166.5) calcd (found): C 70.0 (69.4) H 9.1 (9.1) N 1.2 (1.2). ^{1}H NMR (C_6D_6, 400 MHz) major δ: 7.70 (d, $^4J_{HH}$ 2.4 Hz, 4 H, aryl*H*), 7.43 (d, $^4J_{HH}$ 2.4 Hz, 4H, aryl*H*), 5.30 (q, $^3J_{HH}$ 7.2 Hz, 2 H, bridge-C*H*), 5.06 (m, 4 H, CH_2 of *n*-propyl), 1.72 (m, 4 H, CH_2 of *n*-propyl), 1.58 (s, 36 H, C(CH_3)$_3$), 1.53 (d, $^3J_{HH}$ 7.2 Hz, 6 H, bridge-CH_3), 1.32 (s, 36 H, C(CH_3)$_3$), 0.57 (t, 6 H, $^3J_{HH}$ 6.7 Hz, 6 H, CH_3). Minor δ: 7.52 (d, $^4J_{HH}$ 2.4 Hz, 4 H, aryl*H*), 7.36 (d, $^4J_{HH}$ 2.4 Hz, 4 H, aryl*H*), 5.33 (q, $^3J_{HH}$ 7.2 Hz, 2 H, bridge-C*H*), 5.02 (m, 4 H, CH_2 of *n*-propyl), 1.64 (m, 4 H, CH_2 of *n*-propyl), 1.54 (d, $^3J_{HH}$ 7.2 Hz, 6 H, bridge-CH_3), 1.45 (s, 36 H, C(CH_3)$_3$), 1.23 (s, 36 H, C(CH_3)$_3$), 0.48 (t, 6 H, $^3J_{HH}$ 6.7 Hz, 6 H, CH_3). ^{51}V (C_6D_6, 105.1 MHz) δ: –448.00 ($\omega_{1/2}$ 270), minor peaks at –289.46 ($\omega_{1/2}$ 440), –498.83 ($\omega_{1/2}$ 160).

Synthesis of [VOL^1]$_2$·3(MeCN) (8). [V(N*p*-tolyl)(O*n*-Pr)$_3$] (0.62 g, 1.87 mmol) and L^1H_3 (1.00 g, 1.70 mmol) were refluxed in toluene (40 mL) for 12 h. Upon cooling the volatiles were removed *in vacuo* and the residue extracted into acetonitrile affording **8**·3(MeCN) as dark blocks. Yield: 0.96 g, 79%. M.p. 118 °C. $C_{80}H_{110}O_8V_2$ (sample dried *in vacuo* for 12 h, –3MeCN, 1301.63) calcd (found): C 73.8 (73.7) H 8.5 (8.5). ^{1}H NMR ($CDCl_3$, 300 MHz) δ: 7.32–6.29 (12 H, overlaying signals, Ar–*H*), 4.38 (2 H, d, $^2J_{HH}$ 14.5 Hz, CH_2), 4.13 (2 H, d, $^2J_{HH}$ 14.5 Hz, CH_2), 3.86 (2 H, d, $^2J_{HH}$ 14.4 Hz, CH_2), 3.56 (2 H, d, $^2J_{HH}$ 14.4 Hz, CH_2), 1.48–1.17 (90 H, overlaying signals, *t*-Bu). ^{51}V (C_6D_6, 105.1 MHz) δ: –498 ($\omega_{1/2}$ 340). *m*/*z* (MALDI): 651 (M^+/2). IR (cm^{-1}): 1596 m, 1409 m, 1362 m, 1260 m, 1224 m, 1199 m, 1158 m, 1095 bs, 1014 bs, 924 m, 904 m, 881 m, 858 m, 799 s, 730 m, 687 w, 660 w.

Synthesis of {[V(μ$_2$-O)(N*p*-tolyl)][VO(O*i*-Pr)]L^2}$_2$·1.5(MeCN) (9). [V(N*p*-tolyl)(O*i*-Pr)$_3$] (1.35 g, 4.04 mmol) and L^2H_3 (1.00 g, 1.84 mmol) were refluxed in toluene (40 mL) for 12 h. Upon cooling the volatiles were removed *in vacuo* and the residue extracted into acetonitrile affording **9**·1.5(MeCN) as red prisms. Yield: 0.57 g, 32%. M.p. 219 °C (decomposition). $C_{94}H_{126}O_{12}N_2V_4$ (sample dried *in vacuo* for 12 h, –1.5MeCN, 1679.80) calcd (found): C 67.2 (67.1), H 7.6 (7.7) N 1.7 (1.7). ^{1}H NMR ($CDCl_3$, 300 MHz) δ: 7.50–6.60 (12 H, overlaying signals, Ar–*H*) 6.46 (4 H, d, $^3J_{HH}$ 8.3 Hz, tolyl-*H*), 6.06 (4 H, d, $^3J_{HH}$ 8.3 Hz, tolyl-*H*), 5.74 (2 H, d, $^2J_{HH}$ 16.8 Hz, CH_2), 5.22 (2 H, sept, $^3J_{HH}$ 8.0 Hz, O*i*-Pr), 4.09 (2 H, d, $^2J_{HH}$ 16.8 Hz, CH_2), 3.48 (2 H, d, $^2J_{HH}$ 16.8 Hz, CH_2), 3.39 (2 H, d, $^2J_{HH}$ 16.8 Hz, CH_2), 2.11 (3 H, s, Me), 2.07 (3 H, s, Me), 1.92 (3 H, s, Me), 1.85 (3 H, s, Me), 1.48 (12 H, bs, O*i*-Pr), 1.41 (18 H, s, *t*-Bu), 1.35 (9 H, s, *t*-Bu), 1.31 (9 H, s, *t*-Bu), 1.24 (9 H, s, *t*-Bu), 1.23 (9 H, s, *t*-Bu), 1.21 (9 H, s, *t*-Bu), 1.17 (9 H, s, *t*-Bu). ^{51}V (C_6D_6, 105.1 MHz) δ: –452 ($\omega_{1/2}$ 310), –515 ($\omega_{1/2}$ 487). *m*/*z* (FAB): 1623 (M^+ – O*i*-Pr), 1540 (M^+ – VO_3*i*-Pr), 1524 (M^+ – VO_4*i*-Pr), 1508 (M^+ – VO_5*i*-Pr). IR (cm^{-1}): 1461 s, 1401 s, 1377 s, 1259 m, 1225 m, 1202 m, 1160 m, 1108 m, 1005 m, 920 m, 877 m, 868 m, 849 m, 796 m, 776 m, 625 m, 595 m.

Crystallography

For each sample, a crystal was mounted in oil on a glass fibre and fixed in the cold nitrogen stream on an automated CCD diffactometer equipped with Mo Kα radiation and a graphite monochromator, except for **4**·MeCN and **9**·1.5MeCN which were measured at Daresbury Laboratory SRS Stations 16.2 SMX and 9.8, respectively. Intensity data were measured by thin-slice

Table 12 Crystallographic data

Compound	**2**	**3**·6(MeCN)	**4**·MeCN	**5**	**6**·4(MeCN)	**7b**·2(MeCN)	**8**·3(MeCN)	**9**·1.5(MeCN)
Formula	$C_{11}H_{16}Cl_3N_3OV$	$C_{56}H_{82}O_8S_2V_2$, $6(C_2H_3N)$	$C_{56}H_{80}O_8S_2V$, C_2H_3N	$C_{63}H_{96}O_8V_2$	$C_{60}H_{90}O_8V_2$, $4(C_2H_3N)$	$C_{66}H_{102}O_8V_2$, $2(C_2H_3N)$	$C_{80}H_{110}O_8V_2$, $3(C_2H_3N)$	$C_{94}H_{126}N_2O_{12}V_4$, $1.5(C_2H_3N)$
FW/g mol^{-1}	363.56	1295.54	1037.31	1083.28	1205.42	1207.46	1424.8	1741.31
Crystal system	Monoclinic	Orthorhombic	Triclinic	Monoclinic	Triclinic	Triclinic	Monoclinic	Triclinic
Space group	$P2_1$	$Pbca$	$P\bar{1}$	$I2/a$	$P\bar{1}$	$P\bar{1}$	$C2/c$	$P\bar{1}$
a/Å	8.6892(4)	16.4675(5)	17.2685(19)	15.2469(7)	10.5991(7)	12.5074(4)	15.5098(8)	14.821(3)
b/Å	7.7891(4)	15.2783(5)	19.079(2)	24.3672(11)	12.9675(8)	15.8414(7)	19.2536(11)	17.649(3)
c/Å	11.8673(6)	29.5448(9)	19.842(2)	18.2970(8)	14.7112(9)	17.6437(7)	28.7880(17)	22.129(4)
α/°	90	90	112.4270(16)	90	71.2558(10)	88.361(3)	90	80.787(3)
β/°	102.2408(8)	90	98.4624(17)	108.4160(7)	74.5933(10)	84.915(3)	93.323(4)	76.259(3)
γ/°	90	90	98.2682(17)	90	68.2679(10)	87.381(3)	90	68.612(3)
V/Å^3	784.93(7)	7433.3(4)	5832.8(11)	6449.6(5)	1753.73(19)	3477.4(2)	8582.2(8)	5218.1(16)
Z	2	4	4	4	1	2	4	2
T/K	150(2)	150(2)	150(2)	150(2)	150(2)	140(2)	180(1)	150(2)
Radiation, λ/Å	0.71073	0.71073	0.8462	0.71073	0.71073	0.71073	0.71073	0.6892
D_{calcd}/g cm^{-3}	1.538	1.158	1.181	1.116	1.141	1.153	1.103	1.108
μ/mm^{-1}	1.137	0.360	0.292	0.338	0.318	0.320	0.269	0.401
Crystal size/mm^3	$0.27 \times 0.26 \times 0.17$	$0.41 \times 0.33 \times 0.12$	$0.23 \times 0.15 \times 0.11$	$0.51 \times 0.26 \times 0.15$	$0.98 \times 0.47 \times 0.45$	$0.30 \times 0.22 \times 0.20$	$0.52 \times 0.51 \times 0.48$	$0.15 \times 0.08 \times 0.05$
$2\theta_{max}$/°	57.72	55.00	66.34	58.18	58.00	50.00	55.00	55.00
Reflections measured	6978	61 637	43 293	28 550	15 504	55 721	52 327	50 900
Unique reflections, R_{int}	3610, 0.0189	8500, 0.0415	23 814, 0.0369	7835, 0.0203	8073, 0.0169	12 205, 0.1191	9782, 0.050	25 941, 0.0337
Reflections with $F^2 > 2\sigma(F^2)$	3513	6221	18 131	6188	6816	7084	7118	17 505
Transmission factors	0.749 to 0.830	0.867 to 0.958	0.936 to 0.969	0.847 to 0.951	0.746 to 0.870	0.535 to 0.938	0.914 to 1.049	0.942 to 0.980
Number of parameters	176	442	1386	387	413	831	460	1106
R_1 [$F^2 > 2\sigma(F^2)$]	0.023	0.044	0.062	0.038	0.037	0.097	0.063	0.044
wR_2 (all data)	0.060	0.131	0.164	0.112	0.104	0.257	0.163	0.118
Largest difference peak and hole (e Å^{-3})	0.39 and –0.21	0.71 and –0.42	1.31 and –0.95	0.34 and –0.45	0.39 and –0.34	1.24 and –0.67	0.62 and –0.43	0.49 and –0.57

ω- or ω- and θ-scans. Data were processed using the CrysAlis-RED,[20] DENZO/SCALEPACK[21] or SAINT[22] programs. The structures were determined by the direct methods routines in the SHELXS[23] or SIR-92[24] programs and refined by full-matrix least- squares methods, on F^2, in SHELXL.[24] The non-hydrogen atoms were refined with anisotropic thermal parameters, except in some disordered groups/solvent molecules of crystallisation. For **2** the absolute structure was reliably determined; Flack parameter $x = -0.029(17)$. For **3**·6MeCN, the acetonitrile including N(3) was disordered over two closely spaced positions; major occupancy 61.1(10)%. Also in **3**·6MeCN, the *tert*-butyl group at C(25) had the methyl groups modelled as disordered over two sets of positions; major occupancy 58.1(6)%. For **5**, the group O(1), C(31), C(32), C(33) was disordered 50/50 across the two-fold axis. In **6**·4(MeCN) the *tert*-butyl group at C(23) had the methyl groups modelled as disordered over two sets of positions; major occupancy 70.7(13)%. In **8**·3MeCN, two *tert*-butyl groups were severely disordered, and the minor component of each could only be successfully modelled using isotropic thermal parameters. The *tert*-butyl group at C(41A) had the methyl groups modelled as disordered over two sets of positions, major occupancy 80%; the *tert*-butyl group at C(41B) had the methyl groups modelled as disordered over two sets of positions; major occupancy 53.7(7)%. In **9**·1.5MeCN, one of the acetonitrile molecules per unit cell was badly disordered, and was modelled using the PLATON SQUEEZE procedure.[25] SQUEEZE recovered 27 electrons per unit cell in one void *cf.* 22 electrons for one MeCN molecule, therefore 0.5 MeCN per molecule of the complex. The methyl groups on the *tert*-butyl group at C(48) were disordered over two sets of positions modelled with restraints on geometry and anisotropic displacement parameters; major occupancy: 81.6(5)%. Scattering factors for neutral atoms were taken from reference 26. Crystal data and refinement results are collated in Table 12.

Acknowledgements

The EPSRC is thanked for financial support and the award of beam time at the Daresbury Laboratory and Station Scientists Dr J. E. Warren and Dr S. J. Teat are thanked for their support. We thank Dr Shigekazu Matsui and Mr Sadahiko Matsuura of Mitsui Chemical Inc., Chiba, Japan for the screening of complex **3**. The Mass Spectrometry Service Centre, University of Wales, Swansea is thanked for data.

References

1 (*a*) See for example: H. Hagen, J. Boersma and G. van Koten, *Chem. Soc. Rev.*, 2002, **31**, 357; (*b*) S. Gambarotta, *Coord. Chem. Rev.*, 2003, **237**, 229; (*c*) C. Lorber, F. Wolff, R. Choukroun and L. Vendier, *Eur. J. Inorg. Chem.*, 2005, 2850; (*d*) G.-J. M. Meppelder, T. S. Halbach, T. P. Spaniol, R. Mülhaupt and J. Okuda, *J. Organomet. Chem.*, 2009, **694**, 1235.

2 (*a*) C. Redshaw, L. Warford, S. H. Dale and M. R. J. Elsegood, *Chem. Commun.*, 2004, 1954; (*b*) C. Redshaw, M. A. Rowan, D. M. Homden, S. H. Dale and M. R. J. Elsegood, *Chem. Commun.*, 2006, 3329; (*c*) C. Redshaw, M. Rowan, L. Warford, D. M. Homden, A. Arbaoui, M. R. J. Elsegood, S. H. Dale, T. Yamato, C. Pérez Casas, S. Matsui and S. Matsuura, *Chem.–Eur. J.*, 2007, **13**, 1090; (*d*) D. M. Homden, C. Redshaw and D. L. Hughes, *Inorg. Chem.*, 2007, **46**, 10827; (*e*) D. M. Homden, C. Redshaw, J. A. Wright, D. L. Hughes and M. R. J. Elsegood, *Inorg. Chem.*, 2008, **47**, 5799.

3 (*a*) For early use of ETA see: A. Gumboldt, J. Helberg and G. Schleitzer, *Makromol. Chem.*, 1967, **101**, 229; (*b*) D. L. Christman, *J. Polym. Sci., Part A*, 1972, **10**, 471; (*c*) E. Addison, A. Deffieux, M. Fontanille and K. Bujadoux, *J. Polym. Sci., Part A*, 1994, **32**, 1033.

4 (*a*) Y. Nakayama, H. Bando, Y. Sonobe, Y. Suzuki and T. Fujita, *Chem. Lett.*, 2003, **32**, 766; (*b*) Y. Nakayama, H. Bando, Y. Sonobe and T. Fujita, *J. Mol. Catal. A*, 2004, **213**, 141; (*c*) Y. Nakayama, H. Bando, Y. Sonobe and T. Fujita, *Bull. Chem. Soc. Jpn.*, 2004, **77**, 617.

5 A. K. Tomov, V. C. Gibson, D. Zaher, M. R. J. Elsegood and S. H. Dale, *Chem. Commun.*, 2004, 1956.

6 (*a*) G. J. P. Britovsek, V. C. Gibson and D. F. Wass, *Angew Chem., Int. Ed.*, 1999, **38**, 428; G. J. P. Britovsek, V. C. Gibson and D. F. Wass, *Angew Chem.*, 1999, **111**, 448; (*b*) V. C. Gibson and S. K. Spitzmesser, *Chem. Rev.*, 2003, **103**, 283; (*c*) V. C. Gibsonand E. L. Marshall, in *Comprehensive Coordination Chemistry II*, ed. J. A. McCleverty, T. J. Meyer and M. D. Ward, Elsevier, 2004, vol. 9.

7 (*a*) K. Nomura, A. Sagara and Y. Imanishi, *Chem. Lett.*, 2001, **30**, 36; (*b*) W. Wang, J. Yamada, M. Fujiki and K. Nomura, *Catal. Comm.*, 2003, **4**, 159; (*c*) W. Wang and K. Nomura, *Adv. Synth. Catal.*, 2006, **348**, 743.

8 K. Takaoki and T. Miyatake, *Macromol. Symp.*, 2000, **157**, 251.

9 (*a*) C. R. Cornman, K. M. Geiser-Bush and J. W. Kampf, *Inorg. Chem.*, 1999, **38**, 4303; (*b*) T. P. Paine, T. Weyhermüller, L. D. Slep, F. Neese, E. Bill, E. Bothe, K. Wieghardt and P. Chaudhuri, *Inorg. Chem.*, 2004, **43**, 7324.

10 Z. Janas, D. Wiśniewska, L. B. Jerzykiewicz, P. Sobota, K. Drabent and K. Szezegor, *Dalton Trans.*, 2007, 2065.

11 M. Arndt-Rosenau, M. Hoch, J. Sundermeyer, J. Kipke, and X. Li, *US. Pat.*, 01 304 551, 2003.

12 See for example K. H. Thompson and C. Orvig, *Coord. Chem. Rev.*, 2001, **219–221**, 1033.

13 (*a*) R. Dinda, P. Sengupta, S. Ghosh and T. C. W. Mak, *Inorg. Chem.*, 2002, **41**, 1684; (*b*) M. Sutradhar, G. Mukherjee, M. G. B. Drew and S. Ghosh, *Inorg. Chem.*, 2006, **45**, 5150; (*c*) R. Dinda, P. Sengupta, M. Sutradhar, T. C. W. Mak and S. Ghosh, *Inorg. Chem.*, 2008, **47**, 5634.

14 P. J. Toscano, E. J. Schermerhorn, C. dettelbacher, D. Macherone and J. Zubieta, *J. Chem. Soc., Chem. Commun.*, 1991, 933.

15 C. Redshaw, D. M. Homden, M. A. Rowan and M. R. J. Elsegood, *Inorg. Chim. Acta*, 2005, **358**, 4067.

16 (*a*) E. A. Maatta, *Inorg. Chem.*, 1984, **23**, 2560; (*b*) D. D. Devore, J. D. Lichtenhan, F. Takusagawa and E. A. Maatta, *J. Am. Chem. Soc.*, 1987, **109**, 7408.

17 M. Lutz, H. Hagen, A. M. M. Schreurs, A. L. Spek and G. Van Koten, *Acta Crystallogr., Sect. C: Cryst. Struct. Commun.*, 1999, **55**, 1636.

18 (*a*) S. Pastor, J. D. Spivack and P. L. Steinhuebel, *Heterocycl. Chem.*, 1984, **21**, 1285; (*b*) T. K. Prakasha, R. O. Day and R. R. Holmes, *J. Am. Chem. Soc.*, 1993, **115**, 2690; (*c*) J. Okuda, S. Fokken, H.-C. Kang and W. Massa, *Polyhedron*, 1998, **17**, 943.

19 Despite repeated elemental analyses for **6**, there was no fit between the experimental and the calculated values.

20 *CrysAlis-CCD and -RED, Oxford Diffraction Ltd.*, Abingdon, UK, 2005.

21 Z. Otwinowski and W. Minor, Processing of X-ray diffraction data collected in the oscillation mode, in *Methods in Enzymology*, ed. C. W. Carter, Jr. and R. M. Sweet, Academic Press, New York, 1997, vol. 276, pp. 307–326.

22 *SAINT software for CCD diffractometers*, Bruker AXS, Inc., Madison, WI, 2001.

23 G. M. Sheldrick, *Acta Crystallogr., Sect. A: Fundam. Crystallogr.*, 2008, **64**, 112.

24 A. Altomare, G. Cascarano, C. Giacovazzo and A. Guagliadi, *J. Appl. Crystallogr.*, 1993, **26**, 343.

25 A. L. Spek, *Acta Crystallogr., Sect. A: Fundam. Crystallogr.*, 1990, **46**, C34.

26 *International Tables for X-Ray Crystallography*, Kluwer Academic Publishers, Dordrecht, The Netherlands, 1992, vol. C, pp. 193, 219 and 500.

